

Crown Ether Substituted Monomeric and Cofacial Dimeric Metallophthalocyanines. 2. Photophysical Studies of the Cobalt(II) and Nickel(II) Variants

A. V. Nikolaitchik[†] and M. A. J. Rodgers*

Department of Chemistry and Center for Photochemical Sciences, Bowling Green State University, Bowling Green, Ohio 43403

Received: April 6, 1999; In Final Form: June 28, 1999

Metallophthalocyanines have been prepared with 18-crown-6 residues at the peripheral benzo sites (McrPc). Metal centers employed have been H₂ (free base), Zn(II), Cu(II), Co(II), and Ni(II). In the present report, the Co(II) and Ni(II) systems are considered; the other three compounds were considered in part 1 of this series of papers. Ultrafast transient absorption spectroscopy was employed to examine the dynamic properties of the excited electronic states of the monomers and dimers. Under pulsed photoexcitation conditions, the most prominent feature in the transient absorption spectrum of all systems studied was a transient bleaching at the ground-state absorption maxima. The time profiles for ground-state repopulation of photoexcited McrPc and McrPcD where M = Co(II) and Ni(II) were best described with double-exponential kinetics with lifetimes of 1.3 and 7.6 ps for CocrPc; 0.8 and 7.2 ps for CocrPcD; 3.2 and 12.8 ps for NicrPc; 2.2 and 24.2 ps for NicrPcD, respectively. An analysis of the kinetic data in the case of the Co(II) and Ni(II) Pc monomers and dimers indicated that the initially formed ¹π,π*-singlet state decayed via parallel processes into either a short-lived ³π,π*-triplet state (absorbing maximally around 540 nm) or a vibrationally hot, electronically excited, metal-centered (d,d) state. A rapid blue spectral shift (τ = 1.3 ps) at the red side of the ground-state bleaching band was attributed to vibrational cooling of this latter state. This very rapid rate of cooling of the vibrationally hot metal state indicates that it may be determined by the rate of energy translocation through the M–N bonds to the π-system, and not into the solvent, viz., an intramolecular process. The repopulation dynamics were shown to be independent of whether excitation was at 400 nm (initial formation of an upper excited state) or at 645 nm (initial formation of the lowest excited state), thus indicating that the internal conversion process, S₂(π,π*) → S₁(π,π*), was occurring within the time resolution of the instrument (ca. 500 fs).

Introduction

The first report of this series¹ concerned crown ether substituted metallophthalocyanines (McrPc) and their cofacial dimers (McrPcD) where the metal substituent was H₂ (free base), Zn(II), or Cu(II). In this second report, photophysical data on the Co(II) and Ni(II) metal-centered variants are presented. In addition, the synthesis of a phthalocyanine complex containing Co(II) and the free base is outlined and preliminary photophysical data are reported. The Co(II) and Ni(II) metal centers have unfilled d-orbitals (Co(II) is d⁷ and Ni(II) is d⁸). When such transition elements are present as the central metals in the π-macrocycles of porphyrins, phthalocyanines, and the like, these orbitals couple with the π-orbital system and provide additional channels for π*-deactivation.

Most photophysical studies that have been performed on macrocyclic π-systems to date have focused on the porphyrin variants. In the early days of picosecond transient absorption spectroscopy (1970s to 1980s), research groups in the U.S.A. and the (then) USSR turned their attention to transition-metal-centered porphyrins, including the Co(II) and Ni(II) systems. Kalyanasundaram² has reviewed these reports. The overall picture arising is that the 4-coordinate species in noncoordinating solvents undergo complete ground-state repopulation in times significantly shorter than 1 ns. With the advent of ultrafast

techniques, significantly greater detail about the excited-state dynamics has been revealed. Thus, Loppnow et al.³ have reported that in benzene solution Co^{II}OEP repopulates the ground doublet state with a lifetime of 12 ± 4 ps, which corresponds to an earlier estimate of 10–20 ps.⁴ Of the two metalloporphyrin systems, the Ni(II) variants have been studied more extensively than the Co(II) systems. For example, Rodriguez and Holten⁵ studied Ni^{II}TPP and Ni^{II}PPDME in noncoordinating solvents and concluded that for both systems the excitation initially deposited in the π-system rapidly becomes associated with a d,d excited state of the metal center. The spectral shifts within the first 20 ps were attributed to the internal vibrational relaxation of this ligand field state. Eventually, the vibrationally cold, electronically excited metal state relaxed to the singlet ground state over several hundred picoseconds. More recently, Eom et al.⁶ investigated the ultrafast dynamics of NiOEP and NiTPP in a series of coordinating and noncoordinating solvents. They concluded that vibrational relaxation occurs within 1 ps and, in coordinating solvents (hexacoordinate Ni), an energy relaxation process occurs over 10–20 ps. Subsequent relaxation to the ground-state surface occurred with a 250 ps lifetime. Moreover, Drain et al.⁷ investigated a Ni(II) tetra-*tert*-butylporphyrin that is distorted from planarity by steric influences. They reported solvent and temperature effects and concluded that the ligand field excited-state lifetime at room temperature varied from a few picoseconds in polar media to several tens of nanoseconds in nonpolar situations. They pointed

[†] Current address: Sensors for Medicine and Science, 12321 Middlebrook Road, Suite 210, Germantown, MD 20874.

out that the planar porphyrins, such as NiTPP, showed virtually no dependence of the d,d-state lifetime on solvent or temperature. The authors interpreted these marked differences in terms of the bulky *tert*-butyl groups forcing the electronically excited state to become polar.

There is a paucity of information on the dynamics of the Co(II) and Ni(II) metallophthalocyanines. One investigation of the excited-state dynamics of CoPc and NiPc in 1-chloronaphthalene solution was reported by Millard and Greene.⁸ These authors showed that the ground-state repopulation dynamics at 670 nm had lifetimes of 2.8 ± 0.2 and 2.1 ± 0.2 ps for NiPc and CoPc, respectively. The authors pointed out that the ground-state bleaching signals for both compounds did not completely recover to the initial zero level.⁸ No absorption spectra were obtained for the transients produced. In the following report, a detailed study of the excited-state dynamics of Co^{II}crPc and Ni^{II}crPc is presented.

As indicated in the preceding paper,¹ the presence of the 18-crown-6 residues at the MPc periphery offers the opportunity to assemble cofacial dimeric MPcs in which both Pc rings contain the same metal atom (homodimers). The Co(II) and Ni(II) homodimers have been assembled, and a study of their excited-state dynamics forms a part of this report. It would also be advantageous to have a convenient way of preparing cofacial dimers in which different metals are contained within the Pc rings. This can be achieved, of course, by adding cesium ions to a 1:1 mixture of the appropriate monomers. However, such a method would produce a mixture of homo- and heterodimers that would be very difficult to separate. Thus, an alternative procedure was sought.

Crown ethers are known to form complexes with variously substituted ammonium ions.⁹ Cram et al.^{10,11} have used this property to design compounds mimicking enzymatic activity in methanol. More recently, this concept has been used to develop photochemical supramolecular switches.¹² Following along this idea, one could expect the formation of a supramolecular dimeric system between an MPc with peripheral crown ether substituents and an MPc with peripheral alkylammonium substituents (Figure 1). In the following pages such an attempt is described and some preliminary photophysical properties of a heterodimer are outlined.

Experimental Section

Materials. Ethanol and methanol (spectrophotometric grade, Aldrich) were refluxed with CaH₂, distilled, and stored over molecular sieves (3 Å, Aldrich). Potassium acetate (99.98%), cesium acetate (99.9%), and benzo-18-crown-6 were purchased from Aldrich. All other reagents were of commercial origin and were used without further purification.

Synthesis of Crown Ether Substituted Phthalocyanines. Metal-substituted 18-crown-6 tetra-substituted phthalocyanines (M = Co(II), Cu(II), Ni(II)) were synthesized by refluxing benzo-18-crown-6 dinitrile¹³ and the appropriate metal acetate in ethylene glycol for 6 h; the procedure used was similar to that described by Kobayashi and Lever.¹⁴ Purification was accomplished by repeated washing of the resulting solid with hot ethanol followed by chromatography on basic alumina with CHCl₃-EtOH (15:1 by volume).

Synthesis of (2,9,16,23-Tetracarboxamidophthalocyanato)cobalt(II) (Co-tamPc). Co-tamPc was synthesized using trimellitic anhydride, urea, CoCl₂, and ammonium molybdate in nitrobenzene according to a procedure previously described.¹⁵

Synthesis of (2,9,16,23-Tetracyanophthalocyanato)cobalt(II) (Co-tnPc). A procedure similar to that described by

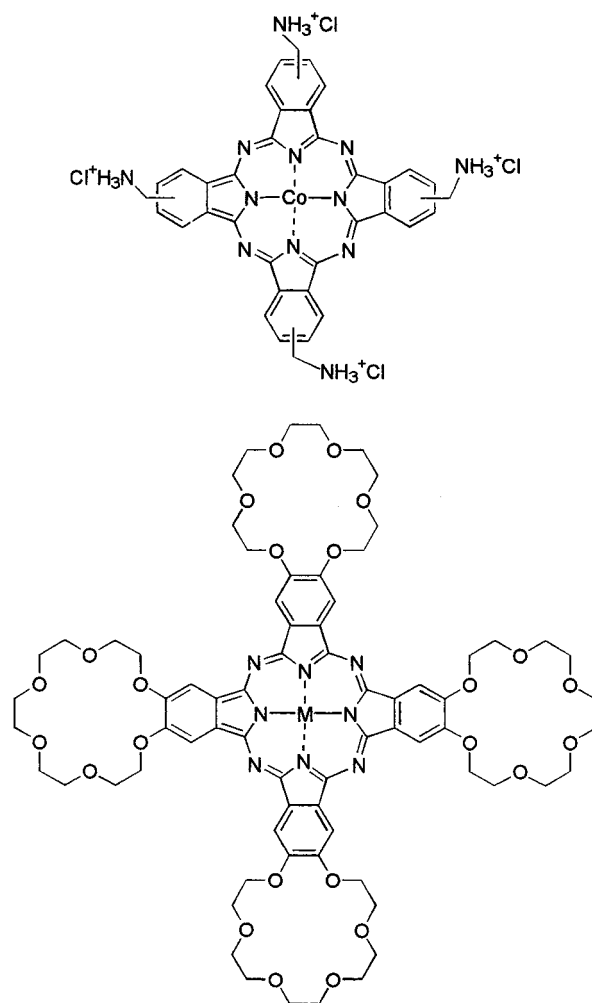


Figure 1. Metallophthalocyanine structures: (upper left) Co(II)-tmacPc; (lower right) an 18-crown-6 substituted metallophthalocyanine.

Lawton and McRitchie¹⁶ was used. Co-tamPc (500 mg, 0.68 mmol) was dissolved in 10 mL of anhydrous DMF; the solution was cooled to 4 °C in an ice/water bath; 2 mL of thionyl chloride (27.2 mmol) was added dropwise with stirring. The ice bath was replaced with an oil bath; the solution was heated to 60 °C and stirred for 16 h at this temperature. The solution was cooled to room temperature and poured onto 100 g of ice. After the ice melted, the mixture was filtered on a fine porosity glass filter. The solid was washed with a copious amount of water and a small amount of acetone and then dried under vacuum at 60 °C. Yield: 72% (330 mg). The IR spectrum of the solid (KBr pellet) indicated complete disappearance of the carboxamide C=O stretching at 1665 cm⁻¹, while the CN stretching appeared at 2226 cm⁻¹. UV-vis (THF): 663 nm (log ϵ = 4.88), 603 nm (log ϵ = 2.22), 331 nm (log ϵ = 4.72). Anal. Calcd for CoC₃₆H₁₂N₁₂: C, 64.38; H, 1.79; N, 25.04. Found: C, 64.03; H, 2.12; N, 24.80.

Synthesis of [2,9,16,23-Tetrakis(methylammonium chloride)phthalocyanato]cobalt(II) (Co-tmacPc). A procedure similar to that reported by Brown et al.¹⁷ was used. Co-tnPc (0.21 g, 0.25 mmol) was placed in 50 mL flask equipped with a reflux condenser. The flask was purged with Ar, and 20 mL of anhydrous, O₂-free THF (distilled from Na-benzophenone) was added while the flask was kept under Ar. The solution was heated to reflux, and 4 mL of 2 M BH₃-SME₂ in THF (Aldrich) was added dropwise. Reflux under Ar was continued for 16 h, and then the solution was poured into a 200 mL beaker; 5 mL of EtOH was added to eliminate the excess of BH₃-SME₂,

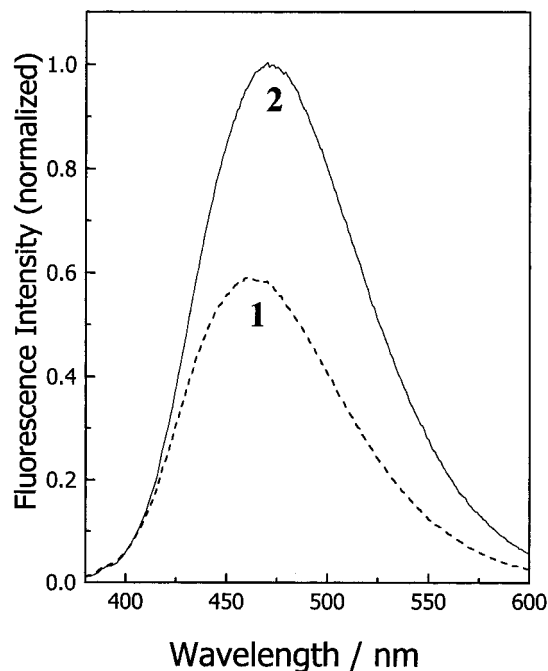


Figure 2. Fluorescence spectra: 1, CocrPc ($\Phi_F = 0.033$); 2, CocrPcD ($\Phi_F = 0.057$). Excitation wavelength was 350 nm.

followed by addition of 1 mL of concentrated HCl in 5 mL of EtOH. The resulting solution was stirred for 3 h. The solid was filtered on a fine porosity glass filter and washed repeatedly with EtOH and CHCl_3 . The dark blue solid obtained was dissolved in 20 mL of H_2O ; the solution was filtered, followed by an addition of 5 mL of 1 N NaOH/ H_2O . This resulted in the precipitation of a blue solid material that was filtered, redissolved, reprecipitated, and refiltered several times. Finally, the solid was combined with 20 mL of MeOH, five drops of concentrated HCl was added, and the solution was stirred for 20 min and filtered. Addition of 10 mL of EtOAc resulted in precipitation of the blue salt, which was filtered off. It was finally purified by ion-exchange chromatography (AG MP-1 resin, Bio-Rad Laboratories). The IR spectrum of the salt (KBr) indicated complete disappearance of the CN groups. UV-vis (EtOH): 675 nm ($\log \epsilon = 4.72$), 329 nm ($\log \epsilon = 4.61$). The compound aggregates in polar solvents. Anal. Calcd: C, 51.86; H, 3.84; N, 20.17. Found: C, 50.79; H, 3.93; N, 18.80.

Procedures. All instrumental procedures used for this work have been described fully in the preceding paper.¹

Results

Steady-State Fluorescence. Ethanol solutions of CocrPc and CocrPcD, upon population of the first excited state (650 nm excitation), showed complete lack of fluorescence. However, significant emission originating from a higher excited state was observed for CocrPc and CocrPcD in EtOH upon excitation at 350 nm; the emission spectra are shown in Figure 2. The quantum yields of this fluorescence emission, referenced to anthracene in ethanol, were determined to be 0.033 and 0.057 for CocrPc and CocrPcD, respectively. The fluorescence excitation spectrum of CocrPc in EtOH containing 1 mM KOAc and recorded with the emission monochromator set at 460 nm resulted in a spectrum identical to the ground-state absorption spectrum in the 300–450 nm region, thereby eliminating the possibility that the observed emission originated from an impurity.

Ultrafast Absorption Spectra and Kinetics. The excited-state dynamics of CocrPc and NicrPc were investigated using

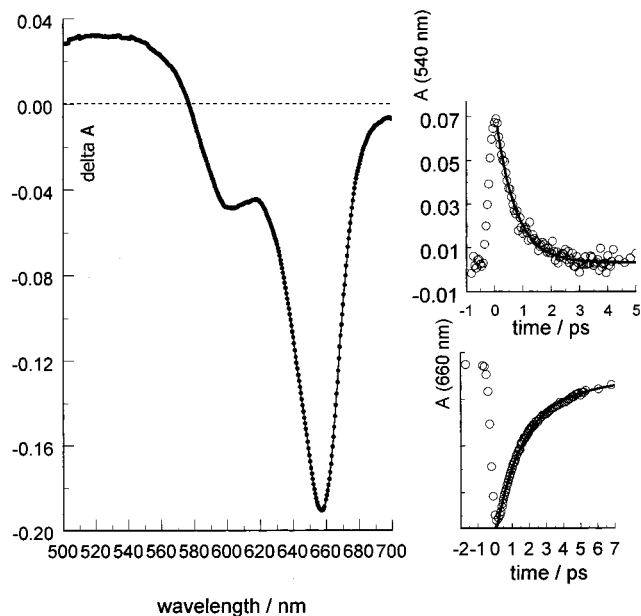


Figure 3. Transient absorption spectra and time profiles for $\text{Co}^{\text{II}}\text{CrPc}$ in ethanol with 1 mM KOAc added and photoexcited at 400 nm. Left panel: spectrum recorded at 1 ps (at 540 nm) after excitation by a 100 fs pulse at 400 nm. Right panels: (upper) time profile and exponential fit ($\tau = 0.9 \pm 0.2$ ps) at 540 nm; (lower) time profile and biexponential fit ($\tau_1 = 1.3 \pm 0.1$ ps; $\tau_2 = 7.6 \pm 0.3$ ps) at 660 nm.

excitation at both 400 nm (B-band absorption) and 645 nm (Q-band absorption). The spectra and kinetic profiles for the ground-state bleaching recovery for both systems were shown to be independent of excitation wavelength. Figure 3 (left panel) shows the absorption spectrum recorded 1 ps after absorption of a 100 fs pulse at 400 nm in CocrPc (5×10^{-5} M) in EtOH. The spectrum shows both positive (around 540 nm) and negative (around 660 nm) absorption segments. Time profiles at the two absorption extrema are shown in the other two panels. Figure 4 displays time-dependent absorption spectra in the region of the ground-state bleaching. The inset to Figure 4 represents times up to 1 ps postpulse onset (see Discussion), and the main figure shows spectra recorded up to 2.5 ps postpulse onset. Figure 5 shows the spectral progression for times up to 34 ps, and Figure 6 shows a plot of the 1.0–2.5 ps spectra (Figure 4) that have been normalized to unit absorbance at 660 nm.

The positive absorption near 540 nm (Figure 3) grew in with the instrument rise time (ca. 500 fs) and decayed with a single exponential having a lifetime of 900 ± 100 fs. The negative absorption signal at 660 nm was formed within the instrumental response of the spectrometer (500 fs), and its recovery (Figure 3) was fitted with a biexponential function that yielded time constants of 1.3 ± 0.1 ps (65%) and 7.6 ± 0.3 ps. Kinetic profiles at the blue edge of the negative absorption (< 660 nm) provided time constants that showed no wavelength dependence, while for those collected at the red edge, the fit parameters were wavelength dependent. The set of spectra J through R shown in Figure 4 (main figure) and again in Figure 6 after normalization show that the spectral band narrows with time, especially at the red side of the ground-state bleach. At the end of this process, a positive absorption band at 690 nm had fully developed. The inset to Figure 6 shows that the logarithm of the spectral half-width was linear with time, with a lifetime of 1.3 ps. The spectra in Figure 4 showed no isosbestic point between the negative (660 nm) and the positive (700 nm) absorption bands up to ca. 4 ps postpulse. At later times an

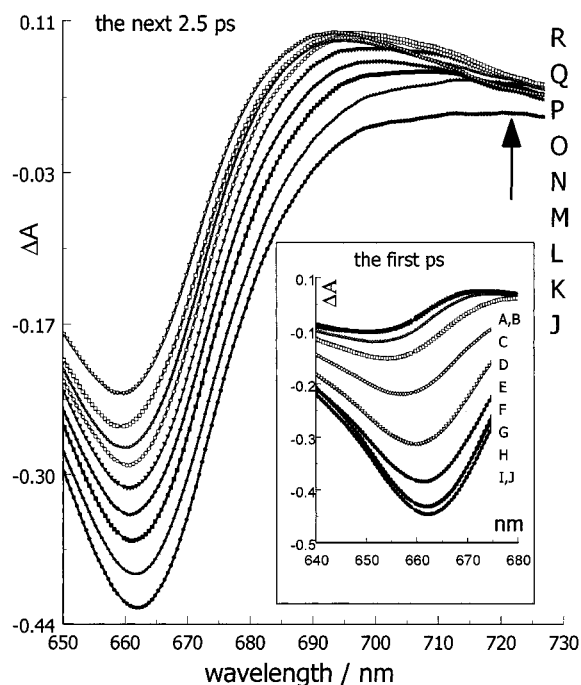


Figure 4. Same experiment as in Figure 3: time-dependent spectra in the 650–730 nm region. (Inset) detail of the first picosecond after excitation: A = -4 ps, B = -2 ps, C = 0.2 ps, D = 0.3 ps, E = 0.4 ps, F = 0.5 ps, G = 0.6 ps, H = 0.7 ps, I = 0.8 ps, J = 0.9 ps. (A and B are superimposed, as are I and J.) Main figure: continuation of the spectra shown in the inset. Spectrum J is at 0.9 ps as in the inset. Subsequent steps are K = 1.2 ps, L = 1.5 ps, M = 1.8 ps, N = 2.1 ps, O = 2.4 ps, P = 2.7 ps, Q = 3.0 ps, R = 3.6 ps.

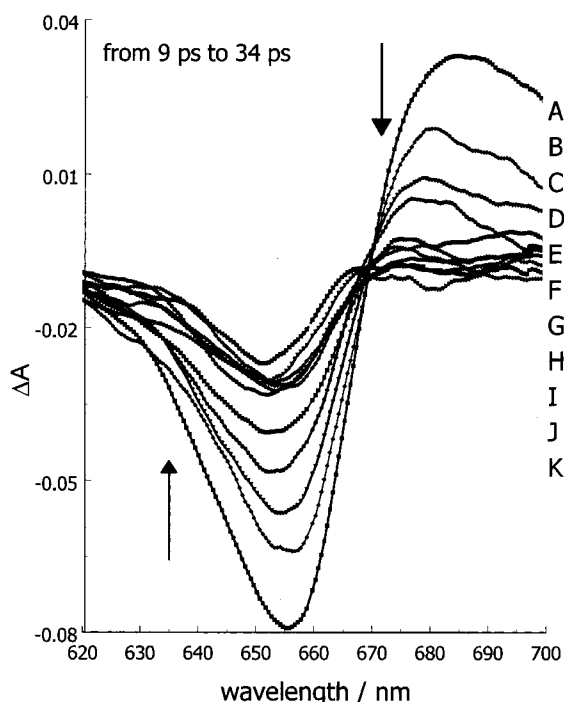


Figure 5. Same experiment as in Figures 3 and 4: continuation of the time sequence up to 34 ps post-pulse. Key: A = 9.0 ps, B = 11.25 ps, C = 13.5 ps, D = 18.0 ps, E = 20.25 ps, F = 22.5 ps, G = 24.75 ps, H = 27.0 ps, I = 29.25 ps, J = 31.5 ps, K = 33.75 ps. The decay of the 690 nm species caused repopulation of the ground state with the generation of an isosbestic point at 670 nm.

isosbestic point developed near 672 nm (Figure 5), indicating that the 700 nm species was decaying with the concomitant repopulation of the ground state.

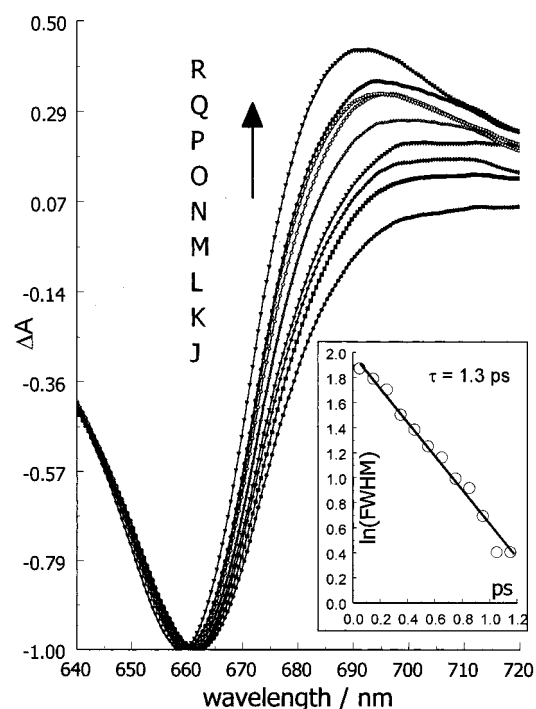


Figure 6. Main figure: same spectra as shown in Figure 4, having been normalized to unit absorbance at the corresponding bleaching minimum. Inset: semilog plot of the fwhm of the bleaching signal vs time.

Experiments similar to those described above performed on NierPc provided similar results. Thus, an ethanolic solution of NierPc (3×10^{-5} M) containing 1 mM KOAc, when excited with 400 or 645 nm pulses, yielded the transient spectrum (at 1 ps postpulse) and the kinetic profiles at 540, 660, and 692 nm shown in Figure 7.

The negative absorbance at 660 nm had a rise time of 500 fs (comparable to the instrument response). Its recovery was described by a double-exponential function with the time constants of 3.2 ± 0.2 ps (45%) and 12.8 ± 0.8 ps. The positive absorbance at 692 nm showed a growth time constant of 1.2 ± 0.3 ps and decay lifetime of 11.9 ± 0.4 ps. The 695 nm-centered transient absorbance displayed significant blue shift as a function of time, with most changes occurring in the first 2 ps postpulse.

A weak, short-lived transient signal at 540 nm (Figure 7) was formed within 500 fs and decayed biexponentially with time constants of 2.8 ± 0.3 ps (95%) and 15.4 ± 0.8 ps. This measurement was performed on a more concentrated sample (1.4×10^{-4} M) for improved S/N. The kinetic parameters extracted from the transient absorbance traces at different wavelengths for monomeric McrPc are summarized in Table 1.

Homodimers. The excited-state dynamics of CocrPcD and NierPcD in EtOH were obtained exactly as for the monomeric systems. Both species showed short-lived positive and negative absorptions that decayed to the prepulse level in a biexponential manner. Typical results for the Ni(II) dimer (4.5×10^{-5} M) are shown in Figure 8. The formation of the 635 and 540 nm signals was complete within the instrumental response time. A double-exponential fit of the negative signal at 635 nm yielded lifetimes of 2.2 ± 0.2 ps (80%) and 24.2 ± 0.2 ps.

An identical experiment conducted for CocrPcD in EtOH showed behavior similar to that of the Ni dimer, differing only in the kinetic parameters. The lifetime details obtained for the excited states of the two cofacial McrPcD dimers are presented in Table 1.

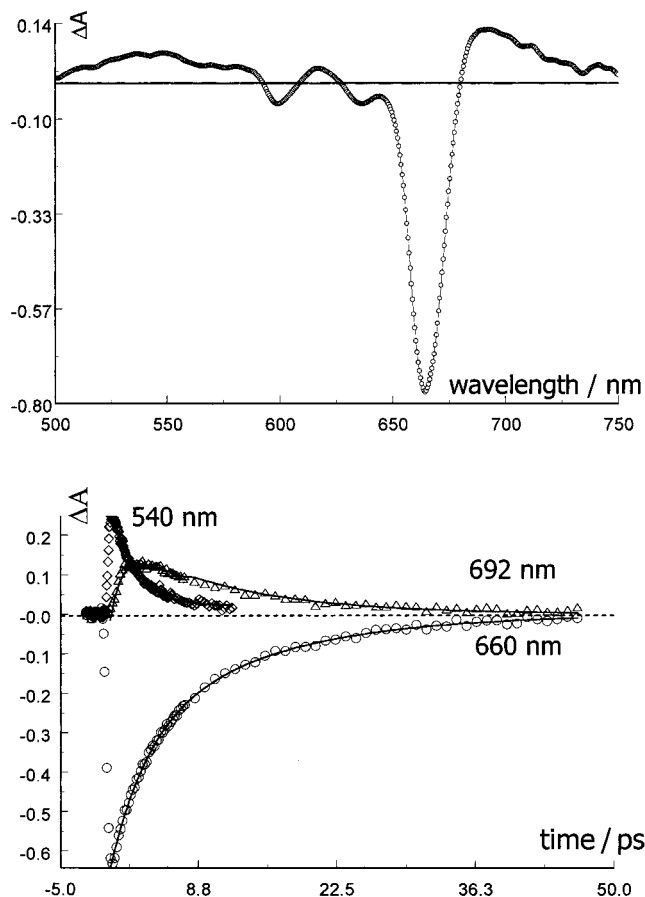


Figure 7. Ni^{II}crPc in ethanol with 1 mM KOAc: transient spectrum at 1 ps (upper panel) and time profiles at 540, 660, and 692 nm (lower panel) for the photoexcited Ni(II) monomer.

TABLE 1: Kinetic Parameters for McrPc Monomers and Dimers

McrPc	λ /nm	τ_1 /ps (%)	τ_2 /ps
CocrPc	540 ^a	0.9 ± 0.2 (90)	8.7 ± 1.7
	660 ^b	1.3 ± 0.1 (65)	7.6 ± 0.6
	700 ^a	2.2 ± 0.4 (50)	8.2 ± 1.4
NiacrPc	540 ^a	2.8 ± 0.4 (95)	15.4 ± 2.0
	660 ^b	3.2 ± 0.3 (45)	12.8 ± 2.1
	692 ^a	11.9 ± 1.5	
CocrPcD	540 ^a	0.5 ± 0.1	
	620 ^b	0.8 ± 0.1 (70)	16.7 ± 0.3
NiacrPcD	540 ^a	2.0 ± 0.2 (70)	21.0 ± 2.4
	635 ^b	2.2 ± 0.2 (80)	24.2 ± 2.6

^a Positive absorption. ^b Negative absorption.

Heterodimer. Solution Characteristics. The synthesis of [2,9,16,23-tetrakis(methylammonium chloride)phthalocyanato]cobalt(II) (Co-tmacPc) was accomplished by using BH₃–SMe₂ in THF to reduce the cyano groups of (2,9,16,23-tetracyanophthalocyanato)cobalt(II) (Co-tenPc). Co-tenPc was synthesized from (2,9,16,23-tetracarboxamidophthalocyanato)cobalt(II) using SOCl₂ in DMF (details in the Experimental Section). Co-tmacPc was soluble in anhydrous EtOH and MeOH where the UV–vis spectrum showed it present as a monomer. Several days after preparation of the solution in methanol, its spectrum displayed changes characteristic of aggregation (band broadening and blue shift). This cationic Pc dye showed good solubility in H₂O where the UV–vis spectra indicated it to be significantly aggregated. Figure 9 shows the absorption spectrum of Co-tmacPc in methanol (spectrum 1 at 2.6 × 10⁻⁵ M) and that resulting from adding solid H₂crPc to the solution (spectrum 2).

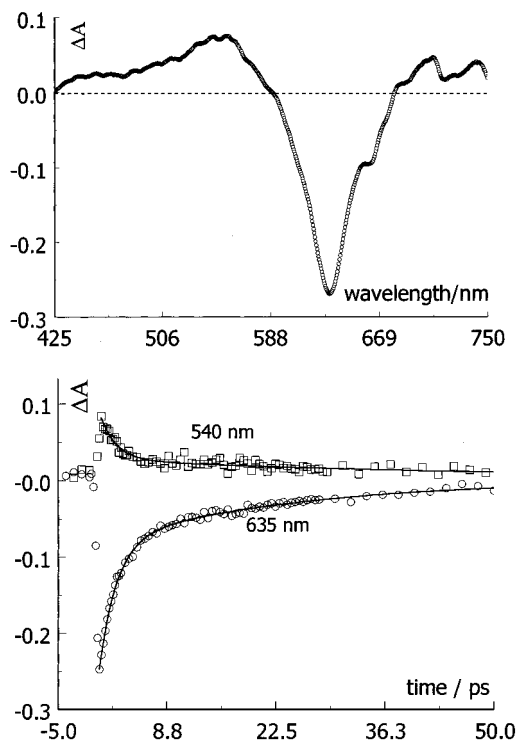


Figure 8. Ni^{II}crPc in ethanol with 1 mM CsOAc: transient spectrum at 700 fs (upper panel) and time profiles at 540 and 635 nm for the photoexcited Ni(II) dimer.

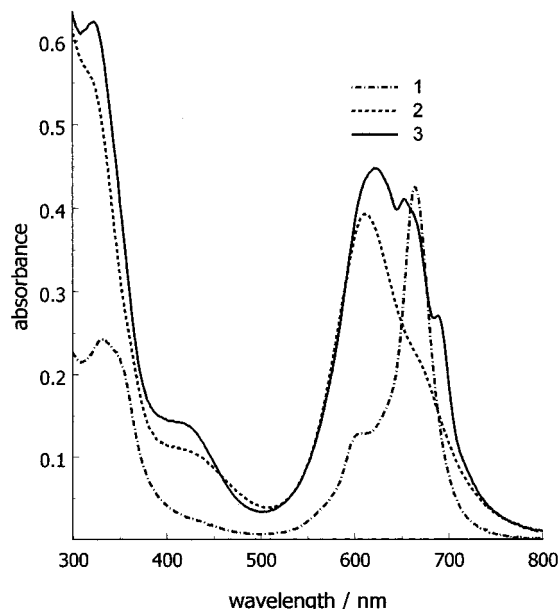


Figure 9. Ground-state absorption spectra in the mixed metal complex experiment: (1) Co-tmacPc (26 μM) in methanol; (2) as for (1) shaken with solid H₂crPc; (3) addition of 1 mM KOAc to same solution causing breakup of the heterodimer.

The very low solubility of H₂crPc in anhydrous methanol (ca. 1 × 10⁻⁶ M) was dramatically enhanced by the presence of Co-tmacPc, implying the formation of a complex between these compounds. In addition, spectrum 2 in Figure 9 does not represent the sum of spectrum 1 and that of H₂crPc, as would be anticipated if there were no complexation. The blue shift observed between spectra 1 and 2 is characteristic for the conversion of a monomeric MPc into a cofacial dimer.¹³ The indications are, therefore, that spectrum 2 in Figure 9 is the absorption spectrum of the “mixed metal” cofacial dimer composed of H₂crPc and Co-tmacPc in a 1:1 ratio. Furthermore,

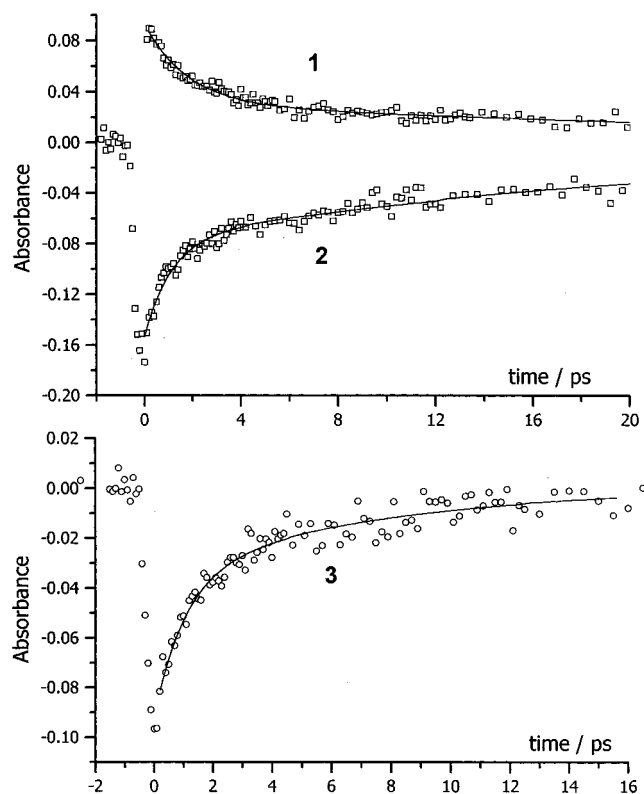


Figure 10. Upper panel: kinetic profiles at 540 nm (1) and 635 nm (2) resulting from photoexcitation of a 26 μM solution of Co-tmacPc in methanol. Lower panel: kinetic profile of the recovery of the ground state following photoexcitation of the heterometal complex under the conditions of spectrum 2 in Figure 9.

it is well established that K^+ ions complex strongly with 18-crown-6 in methanol,¹⁸ and it would be expected that K^+ ions added to the heterodimer solution would compete with the $-\text{NH}_3^+$ groups of the cationic Pc for the crown ether sites of H_2crPc , thereby causing dissociation of the “mixed metal” dimer. Evidence for this is shown in Figure 9 (spectrum 3). Observation of monomeric H_2crPc in methanol in the presence of KOAc has been demonstrated by recent work in this laboratory.¹

Ultrafast Absorption Studies. An ultrafast transient absorption experiment was carried out with Co-tmacPc (2.6 ± 10^{-5} M) in MeOH. The major spectral features were intense bleaching at the wavelength maximum of the ground-state absorption (635 nm) and a positive absorption around 540 nm. Ground-state repopulation showed biexponential kinetics, and fits to the kinetic profiles at 540 and 635 nm yielded lifetimes of $\tau_1 = 1.5 \pm 0.2$ ps (70%) and $\tau_2 = 26 \pm 3$ ps (Figure 10, traces 1 and 2).

In an ultrafast examination of the heterodimer (3×10^{-5} M) in methanol, the bleaching recovery profile recorded at 615 nm (Figure 10, trace 3) was best fit with a biexponential function yielding $\tau_1 = 0.9 \pm 0.2$ ps (60%) and $\tau_2 = 6.8 \pm 0.8$ ps. Thus, the excited-state dynamics are similar to those of the monomeric Co-tmacPc, but somewhat more rapid.

Discussion

The observation of a relatively intense emission from a higher excited state of CocrPc and CocrPcD (342 nm excitation) is an interesting result. Emission from a higher excited state occurs in the compounds with low vibrational coupling between the first and the second electronic excited state. This condition is often met in the molecules with a large gap between energy levels, azulene being an archetypal example of this case.¹⁹ This

condition is true for the Pc compounds, and weak emissions from higher excited states have been reported for Zn(II)- and H_2 -substituted Pc, with quantum yields on the order of 10^{-3} being measured.¹⁴ The quantum yields for the emission from a higher excited state of CocrPc and CocrPcD obtained in the present study are at least 1 order of magnitude larger than those reported for Zn(II) 15-crown-5 tetra-substituted Pc monomer.¹⁴ This difference may be attributed to the effect of the central metal ion on the vibrational coupling between the energy states, since Co(II) is the only element (known thus far) that causes such high quantum yields of higher excited-state emission.

Transition metals, of which Co(II) and Ni(II) are typical, have unfilled d-orbitals; and when such elements are present as the central metal in the π -macrocycles of porphyrins, phthalocyanines, and the like, these orbitals couple with the π -orbital system and provide additional channels for π^* -deactivation. It has been reported^{4,20} that d^7 (Co(II)) and d^8 (Ni(II)) as central metals in Pc and porphyrin compounds facilitate rapid intersystem crossing from the initially excited $\pi-\pi^*$ -state into a variety of possible states of different spin multiplicity. The lifetimes of the $\pi-\pi^*$ -state have been estimated to be less than 250 fs from the values of the fluorescence quantum yields for these compounds (1×10^{-6}).²¹ The initial intersystem crossing process is followed by rapid radiationless deactivation of the excited states regenerating the ground-state molecules.

An investigation of the excited-state dynamics of uncrowned CoPc and NiPc in 1-chloronaphthalene was conducted by Millard and Greene.⁸ These authors used a single exponential to fit the kinetic traces of the ground-state bleaching recovery at 670 nm, obtaining lifetimes of 2.8 ± 0.2 and 2.1 ± 0.2 ps for NiPc and CoPc, respectively, for repopulation of the ground states. No absorption spectra were obtained for the transients produced. The authors pointed out that the ground-state bleaching signals for both compounds did not completely recover to the initial zero level.⁸

The ultrafast time-resolved absorption spectra recorded here for solutions of CocrPc and NicrPc in ethanol showed many similarities; the only significant differences were in the temporal relaxation of the various spectral features. In the following discussion, CocrPc will be described in detail, with the implication that the behavior of the Ni variant differed only in the reaction time scales. In the early times following the excitation pulse, the spectral features that were observed (Figure 3) were positive absorption differences near 540 and 690 nm, with a strong negative absorption difference band (bleaching) at 660 nm where the ground-state spectrum showed a maximum. The kinetic features shown in Figure 3 are discussed below. Figure 4 (main figure and inset) shows the spectral changes that were observed in the first 3.5 ps after excitation. These are the first picosecond (inset) and the next 2.5 ps (main figure). In the inset, spectrum C was the first one to show a significant negative deflection after a series of superimposed spectra (typified by A and B) that were assigned negative times. Spectrum C was obtained at a delay line setting that represented a 200 fs increment from the immediately preceding superimposed spectrum. This latter was assigned to $t = 0$, and thus spectrum C was given the label 0.2 ps. Thereafter, spectra are presented at 100 fs intervals (D through J, with I and J superimposed in the figure). By this reckoning, the maximum negative amplitude was reached at 0.8 ps (spectrum I). A plot (not shown) of the value of ΔA at 660 nm vs time increment showed a sigmoid form with a 10%–90% rise time of 500 fs. This is regarded as the time response of the instrument and is due to the convolution of the ca. 100 fs excitation pulse with

the chirped probe pulse. The progress of chirp, viz., the dispersion of the velocity of light over the wavelength range, through the optical spectrum is manifested by the red shifting of the maximum bleach amplitude as time evolves from 0.2 to 0.8 ps (Figure 4, spectra C through I).

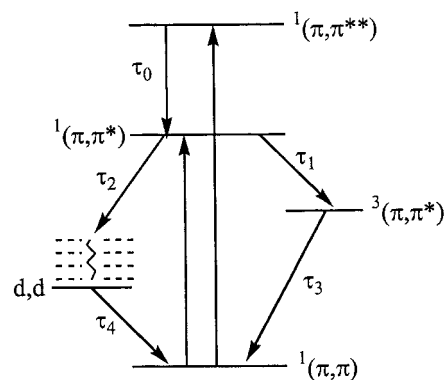
Spectrum J in the main figure is the same as spectrum J in the inset, viz., the 0.9 ps spectrum. During the next 2.5 ps (K through R), the bleaching diminishes as ground states are repopulated, and a positive absorption to the red side of 680 nm grows in. This latter decays in the time interval up to ca. 35 ps (Figure 5), and there is a concomitant repopulation of the ground-state absorption at 660 nm and an intervening isosbestic point at 670 nm (Figure 5). As the positive absorption near 700 nm increases, it undergoes a blue shift (Figure 4, main figure), and a narrowing of the negative absorption band occurs. These latter phenomena can be more clearly seen in Figure 6, in which the main figure shows the same data as in Figure 4 (J through R), now normalized to unit negative absorbance at the relevant λ_{max} . At the half-maximum value, the full extent of the blue shift was 6.5 nm. The inset in Figure 6 shows that the change in half-width is exponential with time, with a lifetime of 1.3 ps. The blue shift is complete by the time of spectrum R in Figure 4 (or 6), and subsequent changes in the 600–700 nm region (Figure 5) are confined to time-dependent concentration changes, as indicated by the appearance of the isosbestic point at 670 nm.

A possible explanation for the spectral blue shifts observed during the first 2.5 ps could be that solvent reorganization around the photoinduced state could be occurring and changing the energy of the optical transition. Such an effect cannot be immediately ruled out since the solvent relaxation time for ethanol has been estimated at less than 10 ps,²² the time regime in which these changes are occurring. To elucidate this point, an ultrafast experiment was conducted with CocrPcD in 1,2-dichloroethane saturated with H₂O and CsOAc. This experiment yielded lifetimes of 0.8 ± 0.1 and 8.5 ± 0.6 ps for the two exponential components of the fit of the ground-state bleaching recovery at 620 nm. These values are virtually identical to those obtained for CocrPcD in ethanol solution (v.i.). Since the solvent relaxation time is less than 2 ps in 1,2-dichloroethane,²³ this result indicates that the observed slow component is unlikely to be connected with solvent dynamics.

In their ultrafast studies of Ni(II) porphyrins, Rodriguez and Holten⁵ and Eom et al.⁶ observed spectral shifts that developed rapidly postpulse. The former authors pointed out that the spectrum that remained after the shifting was complete could be identified as that of a ground-state metalloporphyrin that was different from the initial ground state only by virtue of a different electronic configuration in the metal center. Moreover, both groups concluded that the spectral shifts were arising from vibrational cooling in the metal-centered orbitals. The features reported here for the Co and Ni phthalocyanines can be understood in these same terms. Thus, the blue shift observed at the red side of the bleached Q-band (Figures 4 and 6) is identified as arising from a vibrationally cooling, electronically excited d-state of the McrPc. This cooling process has a lifetime of 1.3 ps, as determined from the rate of decrease of the fwhm of the bleached ground-state band (Figure 6, inset). The fact that no similar TA features to the red of the Q-band bleaching were observed¹ for ZnCrPc and H₂CrPc supports the above assignment proposed for CocrPc and NcrPc.

In this scheme, spectrum R in Figure 4 recorded 2.5 ps after onset (at 660 nm) is the transient difference spectrum of the vibrationally equilibrated, electronically excited CocrPc, in

SCHEME 1



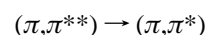
which the electronic excitation resides in the d-manifold in the metal center. As Rodriguez and Holten⁵ asserted for the Ni porphyrins, this has the appearance of a MPc difference spectrum between species having ground-state π -macrocycle configurations slightly modified by a different electronic configuration on the metal center. As time proceeds (Figure 5), the d*-state decays with the concomitant repopulation of the initial ground state of the MPc.

Time profiles of these events in CocrPc are shown in Figure 3. The ground-state recovery (660 nm, lower-right panel) is biphasic, having exponential components of 1.3 ± 0.1 ps (65%) and 7.6 ± 0.3 ps (see Table 1). The lifetime of the d*-state, measured as the decay of the 690 nm absorption, was 8.2 ± 1.2 ps, which is similar to the lifetime of the slower (and lesser) component of the bleaching recovery at 660 nm (Figure 3, lower-right panel). This, together with the observation of the isosbestic behavior, allows the conclusion that the $d^* \rightarrow S_0$ transition has a lifetime of nearly 8 ps for CocrPc. For the Ni variant (see Table 1), a lifetime of ca. 12 ps was measured for this process.

What remains is to assign the larger component of the bleaching recovery having a lifetime of 1.3 ± 0.1 ps (Figure 3, lower-right panel). In this regard, it is noted that the positive absorption band centered at 540 nm (Figure 3, upper-right panel) decays with a lifetime of 0.9 ± 0.2 ps, close to that of the early component of the bleaching recovery. It is likely that the 540 nm transient absorption arises from a triplet state localized on the π -macrocycle and produced rapidly from the initially formed excited state in competition with the formation of the electronically excited d-state. The $^3(\pi, \pi^*)$ -states of metalated phthalocyanines are known to have absorption peaks in the 500–600 nm region.^{24–26} Both CocrPc and NcrPc (Figure 7) showed rapidly decaying absorption features in this spectral region, the lifetimes for which were found to be 0.9 ± 0.2 ps (CocrPc) and 2.8 ± 0.3 ps (NcrPc). These lifetimes were in good agreement with the lifetimes of the fast component of the ground-state recovery profiles. The kinetic data obtained for NcrPc are presented in Figure 7, and the results are collected in Table 1.

The above observations and resulting arguments lead to a proposed kinetic scheme for the excited-state dynamics of NcrPc and CocrPc involving two parallel channels for arriving at the ground-state configuration (Scheme 1).

The dynamic processes labeled in Scheme 1 can be identified with the data as follows. The τ_0 parameter is clearly very small since excitation by blue light (into the upper excited state) was shown to produce the same zero time results as excitation with red light (into the lower state). Thus, internal conversion



occurs within the time resolution of the instrument (ca. 500 fs,) establishing that the above process is more rapid than this interval. Similarly, the data show that the 540 nm absorption bands for both CoCrPc and NiCrPc, assigned to the corresponding $^3(\pi,\pi^*)$ -states, were formed within the instrument response time. Thus, the decay of the $^1(\pi,\pi^*)$ -state by the sum of the processes labeled τ_1 and τ_2 is complete within the instrument response time. The subsequent cooling of the vibrationally excited d^* -state has a rate constant of $0.76 \times 10^{12} \text{ s}^{-1}$, as measured by the rate of change of the spectral width of the ground-state bleaching band (Figure 6, inset). The repopulation of the ground state from the two directions gives rise to the lifetimes τ_3 and τ_4 . For CoCrPc, $\tau_3 = 1.3 \pm 0.1 \text{ ps}$ and $\tau_4 = 7.6 \pm 0.3 \text{ ps}$, while for NiCrPc $\tau_3 = 3.2 \pm 0.2 \text{ ps}$ and $\tau_4 = 12.8 \pm 0.4 \text{ ps}$.

The assignment of the process causing the narrowing of the negative absorption in the Co^{II} - and Ni^{II} CrPcs to cooling of a vibrationally hot, electronically excited, metal-centered state requires that the cooling process has a lifetime of 1.3 ps. Such a lifetime is significantly less than the values of ca. 10 ps that have been reported for vibrational cooling of hemes and other porphyrins.^{5,27–30} However, these latter processes represent the transfer of vibrational excitation from the π -framework to the surrounding matrix, be it solvent or protein. The 1.3 ps process occurring in the metallophthalocyanines is probably not this; rather it is the redistribution of excess vibrational energy initially localized in the metal-centered oscillators into the high density of oscillators within the π -bonded framework (cf. ref 6). Such a process is intramolecular, and it is hardly surprising that it is 1 order of magnitude more rapid than an intermolecular one.

Scrutiny of Table 1 shows that the 540 nm absorption time profiles for the $\text{Co}(\text{II})$ and $\text{Ni}(\text{II})$ compounds were not strictly exponential but showed a small amount ($\approx 10\%$) of a longer-lived component. The lifetimes of these slower components showed similarity to those identified with the process labeled τ_4 in Scheme 1, and it is concluded that the weak features are part of the spectrum of a Pc π -system with an electronically excited metal center.

Cofacial Dimers. Double-exponential kinetics of the ground-state repopulation process were observed for the cofacial Pc dimers with $\text{Ni}(\text{II})$ and $\text{Co}(\text{II})$ centers (see Figure 8 and Table 1). As for the monomers above, such observations can be explained by the presence of two parallel reactions participating in the repopulation of the ground state. The transient absorption signal (Figure 8) for Ni^{II} CrPcD centered at 540 nm may be assigned to the $^3(\pi,\pi^*)$ -state, in line with the results for the monomeric systems. The $\text{Co}(\text{II})$ dimer showed a similar transient band around 540 nm, but its decay was extremely rapid (lifetime 500 fs). It seems, therefore, that Scheme 1 can be invoked to represent also the excited-state dynamics of the $\text{Ni}(\text{II})$ and $\text{Co}(\text{II})$ dimers.

The 540 nm absorption time profile of the $\text{Ni}(\text{II})$ dimer showed nonexponential decay. The curve was fitted with a double exponential, of which 30% showed a 21 ps lifetime. As with the monomers (v.s.), this weak feature is probably part of the absorption spectrum of the excited d-metal-centered Pc.

Mixed Dimer. The formation of a heterodimer between Co-tmacPc and H_2crPc in anhydrous methanol is a heterogeneous process since only a trace of H_2crPc is soluble in this solvent. The amount of H_2crPc ($3 \times 10^{-6} \text{ mol}$) determined to be present in a MeOH solution containing $2.6 \times 10^{-6} \text{ mol}$ of Co-tmacPc is consistent with the formation of a 1:1 heterodimer of the two MPc species in solution. However, the formation of higher aggregates cannot be excluded. Literature examples describing 1:1 stoichiometry of the RNH_3^+ -crown ether complexes³¹ lend

some measure of support to the possibility of the dimeric nature of the $\text{Co}-\text{H}_2\text{Pc}$ system introduced here, but a firm conclusion about the structure of the complex is still distant. The paramagnetic nature of $\text{Co}(\text{II})$ rendered an NMR investigation of the $\text{Co}-\text{H}_2\text{Pc}$ system impossible, and an attempt to obtain a $\text{Zn}(\text{II})$ -substituted analogue of Co-tmacPc through the same synthetic route has so far been unsuccessful.

The investigation of H_2crPc alone in ethanol containing 1 mM KOAc reported in the preceding paper¹ showed the lifetime of the first excited state to be $6.0 \pm 0.1 \text{ ns}$, with a fluorescence quantum yield of 0.66. The triplet state of H_2crPc was determined to have a quantum yield of 0.08 ± 0.02 and a lifetime of 179 μs .¹ In the present study, an ultrafast transient absorption experiment was carried out with Co-tmacPc ($2.6 \times 10^{-5} \text{ M}$) alone in MeOH. The major spectral features were intense bleaching at the wavelength maximum of the ground-state absorption (635 nm) and a positive absorption around 540 nm. Ground-state repopulation showed biexponential kinetics, and fits to the kinetic profiles at 540 and 635 nm yielded lifetimes of $\tau_1 = 1.5 \pm 0.2 \text{ ps}$ (70%) and $\tau_2 = 26 \pm 3 \text{ ps}$ (Figure 10, traces 1 and 2). This dynamic behavior is entirely equivalent to that discussed above for the Co^{II} CrPc compound and the same processes are invoked.

In an ultrafast examination of the “mixed metal” complex ($3 \times 10^{-5} \text{ M}$) in methanol, the bleaching recovery profile recorded at 615 nm (Figure 10, trace 3) was best fit with a biexponential function yielding $\tau_1 = 0.9 \pm 0.2 \text{ ps}$ (60%) and $\tau_2 = 6.8 \pm 0.8 \text{ ps}$. Thus, the excited-state dynamics are similar to those of the monomeric Co-tmacPc, but somewhat more rapid. These results clearly show that the dominant deactivating influence in the dimer is the presence of the transition metal ($\text{Co}(\text{II})$) center in one of the π -systems that make up the dimer. The heterodimer of $\text{H}_2\text{crPc}:\text{Co-tmacPc}$ showed complete lack of fluorescence, and no transient absorptions were detected on nanosecond and longer time scales.

While the above data are far from providing a complete characterization of the Pc system described, these results show that this preliminary approach toward a “mixed metal” species can yield a variety of systems of interesting properties. For example, the RNH_3^+ /crown ether combination offers the potential opportunity to assemble mixed metal dimeric systems that can undergo charge separation reactions after photoexcitation. Another possibility is to create a variety of inter-ring distances by using alkylamino linkers of different carbon chain lengths. Efforts are currently underway to obtain a number of related Pc compounds to allow for more thorough characterization of “mixed metal” entities and to study the effect of the central metal on the photophysical properties of these systems.

Acknowledgment. Support for this project was provided by NIH grants GM24235 and CA46281, NSF grant CHE-9601516, and the Center for Photochemical Sciences, Bowling Green State University.

References and Notes

- (1) Nikolaitchik, A. V.; Korth, O.; Rodgers, M. A. J. *J. Phys. Chem.* **1999**, *103*, 7587.
- (2) Kalyanasundaram, K. *Photochemistry of Polypyridine and Porphyrin Complexes*; Academic Press: San Diego, CA, 1992.
- (3) Loppnow, G. R.; Melamed, D.; Leheny, A. R.; Hamilton, A. W.; Spiro, T. G. *J. Phys. Chem.* **1993**, *97*, 8969.
- (4) Tait, C. D.; Holten, D. *Chem. Phys. Lett.* **1983**, *100*, 268.
- (5) Rodriguez, J.; Holten, D. *J. Chem. Phys.* **1989**, *91*, 3525.
- (6) Eom, H. S.; Jeoung, S. C.; Kim, D.; Ha, J.-H.; Kim, Y.-R. *J. Phys. Chem.* **1997**, *101*, 3661.

- (7) Drain, C. M.; Genteman, S.; Roberts, J. A.; Nelson, N. Y.; Medforth, C. J.; Songling, J.; Simpson, M. C.; Smith, K. M.; Fajer, J.; Shelnut, J. A.; Holten, D. *J. Am. Chem. Soc.* **1998**, *120*, 3781.
- (8) Millard, R. R.; Greene, B. I. *J. Phys. Chem.* **1985**, *89*, 2976.
- (9) Pedersen, C. *J. Am. Chem. Soc.* **1967**, *89*, 7017.
- (10) Timko, J. M.; Helgeson, R. C.; Newcomb, M.; Gokel, G. W.; Cram, D. J. *J. Am. Chem. Soc.* **1974**, *96*, 7097.
- (11) Cram, D. J.; Cram, J. M. *Container Molecules and Their Guests*; Royal Society of Chemistry: Cambridge, U.K., 1994.
- (12) Ashton, P. R.; Ballardini, R.; Balzani, V.; Gomes-Lopez, M.; Lawrence, S. E.; Martinez-Diaz, V.; Montali, M.; Piersani, A.; Prodi, L.; Stoddart, F. J.; Williams, D. *J. Am. Chem. Soc.* **1997**, *119*, 10641.
- (13) Sielcken, O. E.; Tilborg, M. M.; Roks, M. F. M.; Hendriks, R.; Drenth, W.; Nolte, R. J. M. *J. Am. Chem. Soc.* **1987**, *109*, 4261.
- (14) Kobayashi, N.; Lever, A. B. P. *J. Am. Chem. Soc.* **1987**, *109*, 7433.
- (15) Shirai, H.; Maruyama, A.; Kobayashi, K.; Hojo, N.; Urushido, K. *Macromol. Chem.* **1980**, *181*, 575.
- (16) Lawton, E. A.; McRitchie, D. D. *J. Org. Chem.* **1959**, *24*, 26.
- (17) Brown, H. C.; Choi, Y. M.; Narasimhan, S. *J. Org. Chem.* **1982**, *47*, 3153.
- (18) Gokel, G. W. *Crown Ethers and Cryptands*; Royal Society of Chemistry: Cambridge, U.K., 1991.
- (19) *Handbook of Photochemistry*; 2nd ed.; Murov, S. L., Carmichael, I., Hug, G. L., Eds.; Marcel Dekker: New York, 1993.
- (20) Antipas, A.; Gouterman, M. *J. Am. Chem. Soc.* **1983**, *105*, 4896.
- (21) Vincett, P. S.; Voigt, E. M.; Rieckhoff, K. E. *J. Chem. Phys.* **1971**, *55*, 4131.
- (22) Rips, I.; Jortner, J. *J. Chem. Phys.* **1987**, *87*, 2090.
- (23) Gennet, T.; Milner, D. F.; Weaver, M. J. *J. Phys. Chem.* **1985**, *89*, 2787.
- (24) Firey, P. A.; Ford, W. E.; Sounik, J. R.; Kenney, M. E.; Rodgers, M. A. J. *J. Am. Chem. Soc.* **1988**, *110*, 7626.
- (25) Ford, W. E.; Rihter, B. D.; Rodgers, M. A. J.; Kenney, M. E. *J. Am. Chem. Soc.* **1989**, *111*, 2363.
- (26) Rihter, B. D.; Kenney, M. E.; Ford, W. E.; Rodgers, M. A. J. *J. Am. Chem. Soc.* **1990**, *112*, 8064.
- (27) Alden, R. G.; Chaez, M. D.; Ondrias, M. R.; Courtney, S. H.; Friedman, J. M. *J. Am. Chem. Soc.* **1990**, *112*, 3241.
- (28) Lingle, R., Jr.; Xu, X.; Zhu, H.; Yu, S. C.; Hopkins, J. B.; Straub, K. D. *J. Am. Chem. Soc.* **1991**, *113*, 3992.
- (29) Henry, E. R.; Eaton, W. A.; Hochstrasser, R. M. *Proc. Natl. Acad. Sci. U.S.A.* **1986**, *83*, 8982.
- (30) Morlino, E. A.; Rodgers, M. A. J. *J. Am. Chem. Soc.* **1996**, *118*, 11798.
- (31) Colquhoun, H. M.; Stoddart, J. F.; Williams, D. J. *Angew. Chem., Int. Ed. Engl.* **1988**, *25*, 487.